



# Research Repository UCD

<b>Title</b>	Development of a direct simple shear apparatus for peat
<b>Authors(s)</b>	Boylan, Noel, Long, Michael (Michael M.)
<b>Publication date</b>	2009-03
<b>Publication information</b>	Boylan, Noel, and Michael (Michael M.) Long. "Development of a Direct Simple Shear Apparatus for Peat." ASTM, March 2009. <a href="https://doi.org/10.1520/GTJ101703">https://doi.org/10.1520/GTJ101703</a> .
<b>Publisher</b>	ASTM
<b>Item record/more information</b>	<a href="http://hdl.handle.net/10197/3073">http://hdl.handle.net/10197/3073</a>
<b>Publisher's statement</b>	This is a preprint of an article published in Geotechnical Testing Journal, 32 (2): 126-138, available at <a href="http://www.astm.org/DIGITAL_LIBRARY/JOURNALS/GEOTECH/PAGES/GTJ101703.htm">http://www.astm.org/DIGITAL_LIBRARY/JOURNALS/GEOTECH/PAGES/GTJ101703.htm</a>
<b>Publisher's version (DOI)</b>	10.1520/GTJ101703

Downloaded 2025-12-04 23:04:10

The UCD community has made this article openly available. Please share how this access benefits you. Your story matters! (@ucd\_oa)



© Some rights reserved. For more information

**ASTM Geotechnical Testing Journal**Noel Boylan<sup>1</sup> & Michael Long<sup>2</sup>**Development of a Direct Simple Shear Apparatus for Peat Soils****Revised:** August 2008**ABSTRACT:**

This paper discusses the design and development of a new direct simple shear (DSS) apparatus for testing peat soils. The apparatus has been designed to test peat at low effective stresses, representative of its in-situ condition and allow the deformation of the specimen to be monitored. This device uses Particle Image Velocimetry (PIV) image analysis techniques to monitor the side of the peat specimen and provide an insight into the behaviour of peat during shearing. A set of comparative tests on remoulded clay have been conducted with another widely used DSS apparatus and has shown both to yield similar undrained strength ratios ( $s_u/\sigma'_{vc}$ ) for a range of stress levels. Application of the apparatus to peat soils is demonstrated by a set of tests on a high water content blanket bog peat. Analysis of these tests using the PIV technique reveals the complex shear strain and volumetric strain behaviour of peat undergoing shearing. Identification of partial slippage of a specimen is also demonstrated through these analyses.

**KEYWORDS:** peats; organic soils; direct simple shear; laboratory testing; image analysis; particle image velocimetry

---

<sup>1</sup> B.E., PhD Student, Geotechnical Engineering, School of Architecture, Landscape & Civil Engineering, University College Dublin, Newstead Building, Richview Campus, Clonskeagh, Dublin 14, Ireland, Phone +353-1-7163235, Fax +353-1-7163297, noel.boyland@ucd.ie

<sup>2</sup> B.E., MEngSc, PhD, Senior Lecturer, Geotechnical Engineering, School of Architecture, Landscape & Civil Engineering, University College Dublin, Newstead Building, Richview Campus, Clonskeagh, Dublin 14, Ireland, Phone +353-1-7163221, Fax +353-1-7163297, mike.long@ucd.ie

## Introduction

Interest in the shear strength of peat soil has been renewed in recent years due to the occurrence of a number of peat slope failures in Ireland during 2003 (Boylan et al. 2008) and the need to assess peat stability for future developments such as wind-farms located on upland peat deposits. In Ireland, current practice for the assessment of the stability of peat deposits is to obtain undrained shear strength ( $s_u$ ) parameters from in-situ vane tests. This is despite known deficiencies of this test in peat due to the interaction of the fibres with the vane, uncertainty of the actual failure surface and compression of the peat ahead of the vane resulting in a modified peat (Helenelund 1967; Landva 1980).

Laboratory testing of peat soils is complicated by the anisotropy brought about by the predominantly horizontally aligned fibres in the peat, difficulties in simulating the low effective stresses encountered in-situ and interpreting failure of the specimen. In clay soils, the direct simple shear (DSS) has been found to be a useful device to unravel the anisotropy of soils. Bjerrum and Landva (1966) showed that the undrained strength ratios ( $s_u/\sigma'_{v0}$ ) measured in the DSS test were lower than those measured in triaxial compression due to the effects of strength anisotropy. Since, the majority of peat slope failures resemble translational planar type failures and peat is an inherently anisotropic material, the direct simple shear apparatus appears to be a more appropriate apparatus for obtaining strength parameters for stability assessments. This paper describes the development of a direct simple shear (DSS) apparatus to test peat soils at their natural water content, structure and appropriate effective stress level. The apparatus has a facility to monitor the deformation of peat during shearing to identify the nature of the deformation, its uniformity and the development of localisations.

### Direct Simple Shear Testing

Direct simple shear (DSS) testing began with the development of an apparatus by Kjellman (1951) to overcome some of the shortcomings of the traditional direct shear box (DS) test which suffers from non-uniform stress distributions throughout the specimen. The DSS test typically consists of a circular specimen, consolidated to a stress level under  $K_0$  conditions. During shearing, a horizontal shear force is applied to the specimen, while a stack of rings surrounding a membrane (Kjellman 1951) or a wire reinforced membrane (Bjerrum and Landva 1966) keeps the cross-sectional area of the test specimen constant. Other devices have been developed which test square specimen and use rigid steel walls to keep the cross-sectional area constant (Roscoe 1953). The aim of all these apparatuses is to apply a simple shear mode of deformation to a soil specimen, but the need for the ends of the specimen to extend during shearing means that complementary shear stresses are not generated on the ends. As a result of this, the shear stress is non-uniform across the top and bottom of the specimen, falling to zero at the corners. The resulting unbalancing couple has to be counteracted by an opposite couple generated by a non-uniform distribution of normal stress on the top and bottom of the specimen surface (Airey et al. 1985). In routine DSS devices, the total horizontal shear stress ( $\tau_h$ ) and total vertical stress ( $\sigma_v$ ) as well as the horizontal deformation normalised by height ( $h_{def}/H$ ) or engineering shear strain ( $\gamma$ ) are monitored during shearing (see Figure 1). Various authors have criticised these devices as they only measure the total vertical normal stress and the total horizontal shear stress on the specimen during shearing and give no idea of the uniformity of these stresses and true stress state in the specimen. To overcome these shortcomings, a number of researchers (Budhu 1979; Airey 1984) have developed apparatuses which surround the test specimen with an array of load cells to measure

the complete state of stress around the specimen. Radiographic techniques were used to monitor lead shot embedded in the test specimen to give a measure of the internal strains, the uniformity of strains and allow the development of ruptures to be monitored (Budhu 1984). Research conducted by Airey and Wood (1987) on kaolin showed that direct simple shear tests in a routine apparatus with only the total horizontal shear stress and total vertical stress measured underestimated the simple shear values measured in an elaborately instrumented apparatus by only 10%. It has been suggested on the basis of experimental results that simple shear tests on clay can be presented with more confidence than those conducted on sand (Airey and Wood 1984).

In clay soils, static undrained DSS tests are often run as constant volume tests due to difficulties preventing leakages from the test specimen. The test is run at a slow rate to prevent the development of pore pressures, while the vertical load on the specimen is continually varied during shearing to maintain a constant height and in turn keep the volume constant. The change in vertical stress which occurs during the shearing is assumed equal to the change in pore water pressure which would have occurred if the test was truly undrained. Dyvik et al. (1987) confirmed this assumption in a comprehensive study of constant volume DSS tests and truly undrained DSS tests on normally consolidated Drammen clay. These tests showed that the stress-strain and effective stress plots measured by both methods are identical for all practical purposes. While this assumption has not been experimentally verified for peat soils, undrained tests on peat are carried out as constant volume tests in the same manner as for clays (Farrell and Hebib 1998; Den Haan and Kruse 2007)

## Development of UCD-DSS

### *Background*

The UCD-DSS of University College Dublin, was designed to satisfy several criteria identified as essential to allow for DSS testing of peat and strength parameters appropriate for stability assessments. Since the unit weight in peat is extremely low, often close to that of water ( $\approx 10.2 \text{ kN/m}^3$ ), the apparent vertical effective stresses ( $\sigma'_{v0}$ ) in peat are extremely low. For instance, for a typical blanket bog of 2m depth, with the water table close to the surface, the vertical effective stress at the base is normally between 2-5kPa depending on the level of the water table. Simulating and maintaining these low levels of stress is not possible with all standard DSS apparatuses, and for this reason much of the knowledge gained about peat strength has been at effective stress levels greater than that encountered in-situ. The UCD-DSS apparatus was designed to consolidate specimens to the low effective stresses representative of the in-situ condition. For practical purposes, vertical stresses less than 3kPa are not feasible due to difficulties maintaining grip of the specimen during shearing.

Determination of the point of failure in laboratory strength tests on peat is also difficult to judge from the stress-strain behaviour of peat. For instance, in triaxial compression tests on peat, it is not uncommon for the deviator stress ( $\sigma_1 - \sigma_3$ ) to continue increasing with increasing axial strain without reaching a peak. If a peak is reached, it is often encountered at high levels of strain ( $>20\%$ ). In the DSS, similar behaviour has been encountered with specimens straining to large shear strains without reaching a clear peak values. For example, Farrell and Hebib (1998) conducted several DSS tests on peat from Raheenmore bog in Ireland and found that no peak value was reached after 20% shear strain. At these high strains, the uniformity of shear strain throughout the specimen may be problematic and a

localisation may have already developed. Airey and Wood (1987) show an example of a test on speswhite kaolin where the shear stress was continuing to increase but inspection of the internal strains of the test specimen showed that a rupture had already developed. After the development of a rupture, simple shear conditions would no longer exist in the test specimen.

As the water content of peat can be extremely high (>1000%) and the material contains varying amounts of fibres, it was a concern that the peat specimen would simply slip at the horizontal boundary at the top or bottom of the test specimen leading to a situation that horizontal shear stress measurements would not be due to shear straining of the test specimen but compression at the ends of the specimen. Prevost and Høeg (1976) have shown using isotropic elastic analyses that the partial slippage of soil at the boundary, greatly disturbs the uniformity of shear and normal stresses in the test specimen and influences the resulting strength parameters. To overcome these difficulties, the UCD-DSS device was designed to allow for visual inspection of the test specimen during shearing to check if it slips at the horizontal boundaries and assess the uniformity of shear strain in the specimen. This would allow the identification of any strain localisations or ruptures in the specimen which could significantly reduce the uniformity of the shear strain. In addition to this, monitoring of the deformation during shearing provides a unique insight into the deformation properties of peat undergoing shearing and enhances our understanding of this material.

#### *Outline of UCD-DSS Apparatus*

The UCD-DSS apparatus was designed to satisfy the criteria outlined above which were deemed essential for testing specimens of peat. The broad outline (see Figure 2)

of the apparatus was developed by VJ TECH LTD. This device was designed to provide the vertical loading to the test specimen and the horizontal deformation. Vertical loading is applied using direct loading of masses into the loading cup beneath the apparatus. To enable the test specimen to be loaded to the low levels of effective stress required, the entire load of the vertical loading system is balanced by a load balance lever beneath the apparatus enabling the required low stresses to be achieved. Horizontal deformation is applied using a geared stepper motor which is capable of applying deformation rates between 0.00001mm/min to 10mm/min. The stepper motor is in turn controlled by an on board microprocessor unit and touch pad control screen. An RS232 port connected to the microprocessor allows the stepper motor to be controlled separately by a PC.

Using the apparatus developed by VJ TECH LTD to provide vertical and horizontal loads, a test specimen assembly to carry out DSS tests was designed and built at University College Dublin (UCD). Figure 3 shows a side view and section diagram of the test assembly that was developed to house the test specimen. To enable the deformation of the test specimen to be monitored during shearing, it was decided to use a square specimen where one side could be monitored by a digital camera for image analysis. The test specimen has plane dimensions of 70mm square and the height of the specimen can be varied from 5mm to 35mm. To connect to the test specimen at the horizontal boundaries, the top cap (1) and base plate (2) have 1.5mm high and 1mm wide square teeth protruding from them. Drainage during consolidation is facilitated by a porous drain (3) in the centre of the base plate. A valve on the fluid line from this drain allows the drainage to be stopped for the shearing stage of a test. During shearing, tests are conducted as constant volume tests where the height of the test specimen is held constant. DeGroot et al. (1991) outlined the various methods to



maintain constant volume during shear and the shortcomings of each method. Manual control of the vertical stress level was employed to maintain constant height in early versions of DSS apparatuses (Bjerrum and Landva 1966) but this method is quite tedious to use. Constant height can also be maintained by a closed loop feedback system between a displacement transducer monitoring the height of the test specimen and an actuator or pneumatic cylinder applying the vertical stress (DeGroot et al. 1991). A constant height can also be achieved by simply locking the top cap height and it requires that any load cell monitoring vertical stress is within the locked environment. The drawback of this method is that any compliance of elements in the locked environment (i.e. top cap, load cell, bearings, specimen base and porous elements) can rebound during shearing and compress the specimen. Therefore, in the design of an apparatus using this technique to keep the specimen height constant, elements within locked environment need to be designed to minimise compliance. The latter method of maintaining constant height was chosen for this apparatus and vertical compliance tests, presented later in this paper where used to check the level of compliance within the locked environment. After consolidation of the test specimen and before shearing commences, the height of the specimen is held constant by locking the height holding nuts (4) above and below a horizontal member connected to the vertical loading assembly. The top cap and vertical load cell are now contained within the locked environment.

The sidewalls (5) of the apparatus are made from a transparent polymethyl methacrylate (PMMA) material to allow a digital camera to monitor the deformation of the side plane of the test specimen. These sidewalls are polished and free of scratches to minimise friction between them and the soil specimen. The end walls (6) of the box have a smooth surface and are connected to the base plate with hinges (7)

fabricated from a stiff plastic material. A small amount of lubrication is applied to the inside faces of the end walls to minimise local shear stresses between the end walls and the specimen during shearing. These hinges have been fabricated by cutting a V notch out of rectangular piece of plastic. By bending the plastic at the thinnest point, it creates a hinge which allows the rotation to occur as close as possible to the corner. The end walls are connected above the level of the top cap by two rigid horizontal bars with rod eye bearings (8) at either end. These rod eye bearings allow the end walls to deform into the simple shear mode of deformation (See Figure 1). The sides of the end walls, top cap and base plate in contact with the side walls have polytetrafluoroethylene (PTFE) seals to prevent leakage from the test specimen during shearing. These seals are lightly coated with petroleum jelly to reduce friction with the side walls. At the corners where the hinges are located and outside the end walls, petroleum jelly is smeared to further prevent leakage. When a horizontal deformation is applied by the stepper motor drive, the base plate displaces along low friction roller bearings (9) and the rigid bars with rod eye bearings (8) above the top cap move horizontally allowing the test specimen to deform into a parallelogram while maintaining zero lateral strain between the end walls.

Throughout a test the total horizontal load is measure by a 0.5 kN load cell (10) while the total vertical load is monitored by a 1.25 kN load cell (11). Both load cells were chosen with low capacities to maximise the accuracy and resolution of measurements. The vertical load cell (11) has been specially fabricated to undergo no bending effects and remain rigid in the working range of the apparatus. This is to ensure that the top cap does not rotate during shearing. During shearing, the vertical load cell will be subjected to a moment generated by the horizontal shear force and this could influence the measurements of the load cell. Therefore, the design of the load cell is

such that it will not be affected by the moment generated by the shear force up to the capacity of the horizontal load cell. The vertical loading ram (12) is also encased in a linear bearing bushing to ensure verticality and rigidity. The vertical load is transmitted to the vertical loading ram by a cross member (13) which carries the load placed in the loading cup shown in Figure 2. The vertical deformation during consolidation is monitored by a linear variable differential transformer (LVDT) (14), while the horizontal deformation during shearing is also measured by a LVDT (15).

## **Deformation Monitoring**

### *Particle Image Velocimetry (PIV)*

The deformation undergone by the peat specimen during shearing is monitored through the transparent sidewall of the apparatus. As the DSS apparatus is a plane strain device, the deformation at the side plane of the specimen should be similar to that undergone throughout the rest of the specimen. It is not being assumed that this deformation is the exact deformation throughout the rest of the specimen, as the soil in this plane may be influenced by the contact with the sidewall. This deformation is monitored using the Particle Image Velocimetry (PIV) image analysis technique (White et al. 2003). PIV uses the texture variation of the soil in a particular plane, monitored by digital still images taken throughout an experiment to track the deformation undergone by the soil in that plane. White et al. (2003) developed software called GeoPIV to implement this technique for geotechnical applications and showed that it could obtain an order-of-magnitude increase in accuracy, precision and measurement array size compared to previous image-based methods of displacement measurement.

Using the GeoPIV software which is implemented in MATLAB<sup>TM</sup>, a mesh of patches is defined on the first image of the series (illustrated in Figure 4) each with co-ordinates  $(u_1, v_1)$ . Using each of these patches as a reference, the software searches for the location of each patch in subsequent images, using cross correlation and sub-pixel interpolation to define the displaced location of the patch  $(u_2, v_2)$ . By following the location of each patch in subsequent images, the deformation throughout the plane can be recorded. It is important that the images can be taken at time intervals such that the deformation which occurs is within the zone which the PIV software searches for the reference patch. If the time interval is too great and the deformation moves the patch outside the search zone, the PIV analysis will result in erroneous deformation measurements. Since the co-ordinates of the patches  $(u_n, v_n)$  are in image-space co-ordinates of pixels, conversion to object-space co-ordinates  $(x_n, y_n)$  in millimetres is required. Using target markers of known object-space co-ordinates, centroiding and close range photogrammetry are used to convert image-space to object-space co-ordinates. Using the object-space co-ordinates, it is possible to define the displacements and strains throughout the plane of observation.

To enable deformation monitoring using this technique, a CANON<sup>TM</sup> Powershot S80 digital camera with a 8 mega-pixel resolution was mounted parallel to the transparent side wall (item (5) in Figure 3) of the test specimen area to capture images throughout the shearing stage of the test. This camera is capable of computer control and images can be taken at fixed time intervals to allow correlation with load cell and LDVT measurements. Black reference dots with white borders were affixed to the outside of the transparent side wall to act as target markers and the object-space co-ordinates of these markers measured. These markers are used for the conversion of image-space  $(u, v)$  to object-space co-ordinates  $(x, y)$ .

### *Precision of PIV with Peat*

Precision is a measure of mutual agreement among individual measurements of the same property. White et al. (2003) showed that the precision of the PIV technique on soil is strong function of the patch size ( $L$ ) expressed in pixels and the content of the image. Validation experiments which involved the controlled rigid-body movement of a planar body of soil below a camera allowed the influence of patch size to be assessed for sand and clay. For clay, it was required to add an artificial texture to the clay surface using a floc material which would improve the contrast (i.e. spatial variation in brightness) and in turn the precision of PIV analyses. As a result of these experiments, the random error present in PIV data ( $\rho_{\text{pixel}}$ ) was estimated using Equation (1)

$$\rho_{\text{pixel}} = \frac{0.6}{L} + \frac{150000}{L^8} \quad (1)$$

As peat soil is often dark brown or black and can have a poor contrast, experiments similar to those carried out by White et al. (2003) were conducted to assess the influence of patch size ( $L$ ) on the precision of PIV analyses of peat and assess whether an artificial texture would be required to improve contrast of this soil. Figure 5 shows a diagram of the experimental setup used, which is similar to the one used by White et al. (2003). The experimental set-up consists of a carriage to hold a peat specimen which is displaced linearly along a track by prescribed displacements using a micrometer. Images of the carriage containing peat are captured using a digital camera fixed above the carriage.

Two different samples of peat, representing the different extremes which are likely to be encountered were used for these experiments. Figure 6 shows a 200 X 200 pixel image of each of the peat specimen's used;

(a) A moderately decomposed sample of peat which had relatively few fibres and would be representative of the poorly contrasting peat.

(b) A fibrous peat with a relatively low level of decomposition which would be representative of a peat of higher contrast.

A specimen of each of these peat types was placed in the carriage before each experiment. The specimen carriage was then displaced by prescribed displacements of 100 $\mu$ m and 50 $\mu$ m by adjusting the micrometer. Images of the peat specimen in the carriage were taken before and after each displacement via remote control of the camera. Since the image scale of this setup corresponded to a scale of 0.04mm/pixel, the prescribed displacements resulted in image-space displacements of approximately 2.5 and 1.25 image-space pixels respectively. PIV analyses were then carried out on each of these experiments using meshes with patch sizes ( $L$ ) of 10, 20, 30, 40, 60 and 80 pixels. For each PIV analysis of a particular patch size and displacement increment, the average displacement of all the patches in the mesh and the standard deviation was calculated.

Figure 7 shows the resulting standard deviations ( $\rho_{\text{pixel}}$ ) in pixels resulting from different patch sizes. For comparison purposes, the trend suggested by Equation 1 is also shown. Compared to the trend suggested by Equation 1, the standard deviations for PIV analyses of peat soils are higher. For a patch size of 10,  $\rho_{\text{pixel}}$  is between 0.73 and 0.89 pixels which is up to 15 times larger than the deviation of 0.06 pixels suggested by Equation 1. The error in PIV analyses on peat does however decrease significantly when patch size is increased. For a patch size of 40 pixels,  $\rho_{\text{pixel}}$  is between 0.032 and 0.075 pixels which is a 2 to 5 fold increase in deviation to that suggested by Equation 1. At the largest patch size of 80 pixels,  $\rho_{\text{pixel}}$  is a maximum of 0.032. While it might be advantageous from a precision point of view to use larger

patches, this reduces the number of measurement points and lessens the detail that can be revealed in areas of high strain gradient (White et al. 2003). Therefore a balance has to be struck between the level of detail required and the number of measurement points.

The different type of peat being examined is also seen to have an effect on the level of deviation, with deviations for the poorly contrasting peat (a) resulting in errors as much as 2.4 times the error for the more contrasting peat (b). This is due to differences in the spatial variation of brightness between the two peat specimens. Differences in standard deviation for different levels of deformation (2.5 or 1.25 pixels) were only significant for patch sizes less than 40 pixels.

While the standard deviations for PIV analyses on peat are higher than those observed in clay and sand by White et al. (2003), they are acceptable when this precision is expressed non-dimensionally. Dividing the pixel deviation by the image width in pixels expresses the precision as a fraction of the field of view (FOV). For a patch size of 60 pixels, the non-dimensional precision would be a maximum of 1/64383 of the FOV. This is significantly superior to the precision of other image based deformation measurement systems (White et al. 2003) and comparable to the precision obtained by other applications of PIV (White and Take 2005).

### **Compliance and Comparison Tests**

In preparation for conducting tests using the UCD-DSS apparatus, a number of compliance tests were conducted to assess the level of compliance correction to be applied to results. In addition to these tests, comparative tests between the UCD-DSS and another commercially available DSS apparatus were conducted on a uniform reconstituted clay sample.

### *Horizontal Compliance*

Friction generated during rotation of the rod eye bearings, interaction between the end walls and base plate with the side walls, and the displacement of the roller bearing beneath the base plate add to the horizontal shear force measured during the shearing of a specimen. To assess this interaction, horizontal compliance tests were run by locking the height of the top cap at 20mm with no specimen in the apparatus and shearing. Figure 8 shows the horizontal shear stress ( $\tau_h$ ) and the horizontal deformation ( $h_{def}$ ) measured during these tests. It can be seen the horizontal compliance increases from 1.5kPa to 2.25kPa at 10mm horizontal deformation. The increase in compliance with increasing deformation is due to the hinges connecting the end walls to the base plate. The horizontal compliance correction ( $\tau_{h-corr}$ ) in kilopascals (kPa) is approximated for data correction purposes by the linear relationship with horizontal deformation ( $h_{def}$ ) measured in millimetres (mm) shown in Equation 2;

$$\tau_{h-corr} = 1.5 + 0.075h_{def} \quad (2)$$

In addition to this, some further compliance will be generated during a test due to the friction between the specimen and the side walls. This portion of friction would be a function of the lateral stress on the side walls at a point in the test and the coefficient of friction between the peat and side walls. However, as the lateral stress is not measured in this device – correction of this portion of horizontal compliance is complicated. Therefore, tests were carried out on different types of peat which will be used in this device at the stress levels they will be consolidated to, to assess the level of this friction. These tests were carried out by placing a peat sample in the apparatus



with the top cap disconnected from the vertical loading ram. A load was placed directly on the top cap and the specimen was displaced between the side walls without a shear deformation being applied to it. This type of test was also carried out without a specimen to measure the friction due to the apparatus alone. These tests were carried out on peat from two sites covering the extremes of peat types which would be tested in this device; Peat 1 (water content,  $w = 250\%$ ) and Peat 2 ( $w = 1350\%$ ) at vertical stresses of 2.3kPa and 4.6kPa.

Figure 9 shows the results of these side wall friction tests. The test conducted without a specimen shows the friction of the apparatus alone to be approximately 1.5kPa. Initially, all of the peat specimens have a significant wall friction which reduces within 4mm of horizontal displacement as the specimen debonds itself from the side walls. For further displacement, all the specimens exert a friction of less than 0.5kPa. The differences between the specimens 'Peat 1' and 'Peat 2' are only slight and the differences between the vertical stresses used are indistinguishable. The low level of friction between the specimen and the side walls is likely due to the soft texture of peat and the lubricating effect of the high moisture contents. To correct for this effect in practice, 0.5kPa will be deducted from the peak  $\tau_h$ . As the peak  $\tau_h$  in DSS tests on peat typically occurs at displacements greater than 4mm for a 20mm high specimen ( $> 20\% \gamma$ ), this level of correction would be appropriate. This correction is only appropriate for peat's similar to those tested, at vertical effective stresses less than 5kPa.

### *Vertical Compliance*

During the loading of a specimen for the consolidation phase of a test, compression of elements in the vertical loading assembly may result in erroneous vertical deformation being measured. During the shearing stage of a test when the height of the specimen is locked, vertical compliance which takes place within the locked environment may rebound and compress the test specimen. It is therefore essential that vertical compliance is as low as possible within this region.

Tests were conducted to assess the level of vertical compliance in the vertical loading system and the amount of the compliance within the locked environment. These tests were carried out to assess the required correction to the vertical deformation ( $v_{\text{def}}$ ) during consolidation and assess the level of compliance which may rebound on the specimen during shearing. The tests were carried out by placing a steel element in place of the test specimen. The apparatus was then incrementally loaded to vertical stresses ( $\sigma_v$ ) of approximately 20, 55 and 100kPa and the vertical deformation ( $v_{\text{def}}$ ) recorded. At each of these stress levels, the top cap height was locked, the masses removed from the loading cup beneath the apparatus and the vertical deformation ( $v_{\text{def}}$ ) again recorded. The measured vertical deformation after removing the load would show the portion of the vertical compliance which is due to elements outside and inside of the locked environment. This is of course assuming that the compliance outside the locked environment behaves elastically.

Figure 10 shows the relationship between vertical stress ( $\sigma_v$ ) and vertical deformation ( $v_{\text{def}}$ ) for the three tests conducted. At the maximum vertical stress of 100kPa, the total vertical compliance is 0.28mm. At this point, the height was locked and the masses unloaded leaving a vertical deformation of 0.067mm due to compliance within the locked environment. At the stress level of 20kPa which is close to the level which the

apparatus has been designed for, total vertical compliance is 0.088mm, of which only 0.018mm is due to compliance within the locked environment. For the three tests conducted, only 25% of the vertical compliance is within the locked environment where it is uncertain how it behaves during shearing. Indeed it would be impossible to remove all the compliance within this locked environment as the vertical load cell requires a deformation to occur to measure a load. Given that peat is extremely soft and the possible rebound is less than 0.1% vertical strain of a typical 20mm high specimen when consolidated to a  $\sigma_v$  less than 20kPa, it is being assumed that this possible rebound would not have a detrimental effect on peat specimens and the vertical stress ( $\sigma_v$ ) measurements. For a stiffer soil, this rebound would be a more significant problem.

The vertical deformation ( $v_{def}$ ) measured in millimetres (mm) which occurs during consolidation is corrected for compliance ( $v_{def-corr}$ ) using the approximation in Equation 3 where  $\sigma_v$  is the vertical stress measured in kilopascals (kPa).

$$v_{def-corr} = -0.00003\sigma_v^2 + 0.0053\sigma_v \quad (3)$$

### *Clay Comparison Tests*

To assess the performance of the UCD-DSS device, particularly in measuring the undrained shear strength ( $s_u$ ), comparative tests with another commercially available DSS apparatus were conducted. Tests were carried out on both the UCD-DSS and a GEONOR<sup>TM</sup> H-12 direct simple shear apparatus which is of the same design as the apparatus used by Bjerrum and Landva (1966) and widely used in geotechnical practice. This apparatus tests a circular specimen of 79.5mm diameter and 19mm

high which in this case is surrounded by a membrane and stack of rings to keep the cross sectional area constant.

The clay used in this study was reconstituted from Macamore clay, a natural clay till from the south east of Ireland. Particles greater than 0.425mm were removed and the distribution shown in Figure 11 was developed. Table 1 shows the basic properties of the resulting soil. Test specimens were consolidated in both apparatuses to vertical effective stress levels ( $\sigma'_{vc}$ ) of approximately 35, 50 and 70kPa. After consolidation, constant volume DSS tests were conducted at a rate of 4% shear strain per hour in both apparatuses. Data from the UCD-DSS was corrected using the compliance corrections discussed in the previous section, while data from the GEONOR<sup>TM</sup> apparatus was corrected using appropriate compliance corrections.

Figure 12(a) shows the horizontal shear stress normalised by the vertical consolidation stress ( $\tau_h/\sigma'_{vc}$ ) for all DSS tests versus the shear strain. It can be seen that the peak normalised shear stresses for all tests lie in the range of 0.27 to 0.41. The stress strain curves from the GEONOR<sup>TM</sup> tests appear to be more variable due to the higher capacity load cell used on the apparatus. Comparing the post-peak behaviour from both apparatuses, there is a tendency for the UCD-DSS to show a lower degree of strain softening than the GEONOR<sup>TM</sup>. The higher degree of strain softening in the GEONOR<sup>TM</sup> may be a result of the small lateral strains occurring in the specimen due to the expansion of the membrane over the inclined stack of rings. Figure 12(b) shows the pore pressure normalised by the vertical consolidation stress ( $u/\sigma'_{vc}$ ) for all DSS tests versus the shear strain. These equivalent pore pressures are calculated from the drop in vertical stress ( $\sigma'_v$ ) during constant volume shearing and are the assumed pore pressures which would have occurred if the tests were truly undrained. The results from both apparatuses are broadly the same, except for one test in the GEONOR<sup>TM</sup>

which has a lower equivalent pore pressure than the other tests. Figure 13 shows the undrained strength ratios ( $s_u/\sigma'_{vc}$ ) calculated from the peak horizontal shear stress for all tests versus the vertical effective consolidation stress ( $\sigma'_{vc}$ ). For comparison purposes, the limits found by Ladd (1991) for normally consolidated soft clays and silts of a plasticity index of 14% are shown. There is strong agreement between  $s_u/\sigma'_{vc}$  values for the two apparatuses with a trend of a decreasing  $s_u/\sigma'_{vc}$  with increasing  $\sigma'_{vc}$ . The cause of this decreasing trend rather than a constant value which would be expected was explained by conducting two constant rate of strain (CRS) oedometer tests. The first test was conducted on the remoulded material at water content similar as in the DSS tests. The second test was conducted on material with an initial water content of 1.5 times the liquid limit (LL) to define the intrinsic compression line (ICL) of the remoulded material (Burland 1990). This comparison indicated (See Figure 14) that for the  $\sigma'_{vc}$  levels at which the specimens were consolidated in the DSS apparatuses, the soil lies to the left of the ICL and is still tending towards it. This would mean that the soil would exhibit the behaviour of an overconsolidated soil until it reaches the ICL, and therefore higher  $s_u/\sigma'_{vc}$  ratios than the normally consolidated material would be observed.

### Example Application

In order to demonstrate the performance of the UCD-DSS, tests were conducted on peat samples to display the results and demonstrate the deformation monitoring during a test.

### *Peat Tested*

The peat tested comes from a blanket bog near Loughrea, Co. Galway in western Ireland. The peat depth at this site ranges from 0.2m to 4.5m deep and lies on slopes ranging from 0° up to 20°. This site was chosen as it is typical of a site where construction of infrastructure projects such as wind farms would take place, requiring geotechnical assessment of the stability of the slopes. Samples were obtained from a location with 4m depth of peat. Shallow peat samples were obtained by pushing thin walled piston tubes into the ground and then excavating the ground around the tube to retrieve it. Table 2 shows the basic properties of the peat tested. The state of decomposition of the peat has been measured using the method of von Post and Granlund (1926) and detailed in Hobbs (1986).

Three DSS tests were conducted on specimens from this site using the UCD-DSS. All specimens had an initial height of 20mm. Specimens were consolidated under  $K_0$  conditions in two stages to in-situ vertical effective stress ( $\sigma'_{vo}$ ) of approximately 4.3kPa and left to consolidate overnight. After consolidation, the specimen height was locked and shearing commenced at a shear strain rate of 4% per hour. During shearing, digital images of the side wall of the test specimen assembly were taken at regular intervals of 0.33% shear strain for PIV analysis. This interval was chosen to allow for a dense mesh of measurement points and ensure that the displaced patches were within the search zone. Raw data was corrected after testing using the compliance corrections discussed earlier.

### *Test Results*

Figure 15(a) shows the horizontal shear stress ( $\tau_h$ ) versus shear strain ( $\gamma$ ) for each of the tests conducted. With the exception of the test DSS-03, the shear stress increases

without reaching a clear peak. In the test DSS-03, a peak horizontal shear stress of 3.4kPa is reached. Figure 15(b) shows the equivalent pore pressure ( $u$ ) versus shear strain ( $\gamma$ ) for all the tests. The results of the three tests are similar.

### *Deformation Monitoring*

After testing, PIV analyses were carried out on all digital images using the GeoPIV software. This section will focus on the analysis of the tests DSS-01 and DSS-02 to demonstrate the information on the deformation of peat which can be gained using this technique. For these analyses, a patch size ( $L$ ) of 60 pixels was used and the areas around the boundaries of the specimens were excluded to prevent erroneous deformations. Figures 16 and 17 show the results for the tests DSS-01 and DSS-02 respectively at two increments of global shear strain ( $\gamma_{xy-g}$ ) measured at the boundary of the specimen. These results are shown in terms of;

- (a) the distribution of cumulative engineering shear strain in the xy plane ( $\gamma_{xy}$ ).
- (b) the maximum incremental shear strain ( $\gamma_{i-max}$ ) distribution during a 1% increment of global shear strain. The maximum incremental shear strain ( $\gamma_{i-max}$ ) is calculated using Equation 4.

$$\gamma_{i-max} = \varepsilon_{1-inc} - \varepsilon_{2-inc} \quad (4)$$

where  $\varepsilon_{1-inc}$  and  $\varepsilon_{2-inc}$  are the principal strains during an increment of deformation (i.e. between successive images). The distribution of  $\gamma_{i-max}$  gives an indication of the mechanism of deformation which is occurring at a particular interval in the overall deformation process. This would assist in identifying if the specimen is undergoing shear strain throughout or if a strain localisation has developed.

(c) the volumetric strain ( $\epsilon_{vol}$ ) distribution which is calculated directly from the direct strains ( $\epsilon_x$ ,  $\epsilon_y$ ) in the x and y directions using Equation 5.

$$\epsilon_{vol} = \epsilon_x + \epsilon_y \quad (5)$$

The results are presented in terms of the normalised height ( $y/H$ ) where  $H$  is the height of the specimen after consolidation.

Examining the distribution of engineering shear strain ( $\gamma_{xy}$ ) for the specimen DSS-01 (Figure 16a), it can be seen that the vast majority of the specimen is undergoing shear strain by 20%  $\gamma_{xy-g}$ . The zones of low  $\gamma_{xy}$  (especially evident at 10%  $\gamma_{xy-g}$ ) may be a result of some adhesion of the specimen to the sidewall during the early stage of the test. Some zones of localised large shear strain are identifiable although these represent a small proportion of the total specimen. Figure 16(b) shows the maximum incremental shear strains ( $\gamma_{i-max}$ ) at the two stages in the test. At both points, the specimen is undergoing shear strain throughout, indicating that the specimen has not slipped at either of the boundaries. By 20%  $\gamma_{xy-g}$ , the majority of the deformation is concentrated towards the centre of the specimen and the lower ( $y/H < 0.5$ ) right hand corner. Figure 16(c) shows the volumetric strain ( $\epsilon_{vol}$ ) at the two stages in the test. It can be seen that although this test is a constant volume test globally, there are significant localised volumetric strains within the specimen. At 10%  $\gamma_{xy-g}$ ,  $\epsilon_{vol}$  ranges predominantly between +/-10% with some small local zones in excess of this. By 20%  $\gamma_{xy-g}$ , the zones of volumetric extension ( $-\epsilon_{vol}$ ) have extended and are predominantly close to where the deformation is concentrated in Figure 16(b). Visual inspection of the specimens showed that these zones of large extension ( $\epsilon_{vol} < -15\%$ ) resulted in some tearing of the peat structure. As the horizontal shear stress ( $\tau_h$ ) is still increasing



while this volumetric extension is occurring (See Figure 15a), it is likely that this is a redistribution of the solid phase of the peat mass to provide resistance to the applied shear stress. Taking into account the increasing non-uniform deformations being observed and the large zones of extension developing in the specimen, it would be prudent to assign failure at some point based on these observations rather than wait for a peak  $\tau_h$  to develop. Further research is required on a range of peats to identify the criteria for assigning failure under these conditions.

Figure 17(a) shows the distribution of engineering shear strain ( $\gamma_{xy}$ ) for the specimen DSS-02. At 10%  $\gamma_{xy-g}$ ,  $\gamma_{xy}$  is concentrated in the lower left hand side of the specimen. By 20%  $\gamma_{xy-g}$ , the upper right hand corner has undergone little or no shear strain. Similarly, the maximum incremental shear strain ( $\gamma_{i-max}$ ) distributions (Figure 17b) reveal the same pattern of the deformation being concentrated in the lower left hand corner. Figure 17(c) shows the volumetric strain ( $\epsilon_{vol}$ ) for the same stages in the test. It is especially evident at 20% global shear strain that the specimen is undergoing compression in the lower left hand corner and extension in the upper right hand corner. The excessive compression and concentration of deformation in the lower left hand corner indicates that the specimen has slipped along the lower boundary. While the horizontal shear stress ( $\tau_h$ ) is increasing throughout this test (See Figure 15), this is due to the compression of the specimen rather than shear straining. Consequently, the result of this test should be omitted from any further analyses.

## Conclusions

A new direct simple shear apparatus has been developed to test peat soils at low effective stresses representative of the in-situ condition. The apparatus uses PIV

image analysis techniques to monitor the deformation of a plane at the side of the specimen during shearing and provide insight into the evolving failure mechanism.

Laboratory trials to assess the precision of PIV with peat have shown that it is applicable to relatively low texture peat soils and can achieve the non-dimensional precision found by other applications of PIV when a patch size greater than 60 is used.

Compliance tests to measure both the horizontal and vertical compliance were described. The level of horizontal compliance can be a large percentage of the measured strength of a peat specimen tested in this device but is a consequence of the need to have a square specimen to allow the deformation to be monitored. In addition to the compliance due to elements in the apparatus, a small portion of friction is generated between the specimen and the sidewalls. To correct for this, it is required to carry out material friction tests with the different peats used at the appropriate vertical effective stress levels.

Comparative tests between the new apparatus and another widely used apparatus have been conducted with remoulded clay specimens. These tests show both apparatus to yield similar undrained strength ratios ( $s_u/\sigma'_{vc}$ ) for a range of stress levels although the post peak behaviour differs. It is likely that the latter difference is due to the different boundary conditions in both apparatuses.

Tests conducted on peat samples have demonstrated the capability of the UCD-DSS to tests specimens consolidated to low effective stresses ( $< 5\text{kPa}$ ). Two of these tests were used to demonstrate the type of information which can be interpreted from the deformation of peat specimens. The test DSS-01 revealed the increasing non-uniformity of shear strains and localised volumetric strains during the shearing of the peat specimen. Analysis of DSS-02 showed the deformation of a specimen which had

slipped at the horizontal boundary resulting in a concentration of shear strain and compression in the lower left hand corner. This information could be used to assign failure based on the excessive non-uniformities or omit a result based on slippage of the specimen. Further research on a wide range of peats is required to identify the criteria for assigning failure with evolving non-uniform deformation.

### **Acknowledgements**

The first author would like to acknowledge RPS Consulting Engineers and the Geotechnical Trust Fund of Engineers Ireland from whom he has received scholarships. The assistance of technicians Frank Dillon and George Cosgrave is gratefully acknowledged. The assistance of VJ Tech Ltd with the production of the apparatus and Prof. David White of the University of Western Australia for his assistance with GeoPIV is also acknowledged. Dr. John Powell of BRE and Dr. Sarah Stallebrass of City University are also acknowledged for lending UCD the GEONOR<sup>TM</sup> DSS apparatus. Thanks are also due to the reviewers for their helpful comments on an early draft. Lastly, the authors are also grateful for the support of the Environmental RTDI Programme 2000-2006, financed by the Irish Government under the National Development Plan and administered on behalf of the Department of the Environment, Heritage and Local Government by the Environmental Protection Agency.

## References

- Airey, D. W. 1984. "Clays in circular simple shear apparatus," PhD thesis, University of Cambridge.
- Airey, D. W., Budhu, M. and Wood, D. M. 1985. "Some aspects of the behaviour of soils in simple shear," *Developments in Soil Mechanics and Foundation Engineering-2*, P. K. Banerjee and R. Butterfield, Elsevier Applied Science Publishers pp. 185-213
- Airey, D. W. and Wood, D. M. 1984. "Discussion on: Specimen size effect in simple shear test," *Journal of Geotechnical Engineering Division ASCE*, Vol. 110, No. 3, pp. 439-442.
- Airey, D. W. and Wood, D. M. 1987. "An evaluation of direct simple shear tests on clay," *Géotechnique*, Vol. 37, No. 1, pp. 25-35.
- Bjerrum, L. and Landva, A. O. 1966. "Direct simple-shear tests on a Norwegian quick clay," *Géotechnique*, Vol. 16, No. 1, pp. 1-20.
- Boylan, N., Jennings, P. and Long, M. 2008. "Peat slope failure in Ireland " *Quarterly Journal of Engineering Geology and Hydrogeology*, Vol. 41, No. 1, pp. 93-108.
- Budhu, M. 1979. "Simple shear deformation of sands," PhD thesis, University of Cambridge.
- Budhu, M. 1984. "Nonuniformities imposed by simple shear apparatus," *Canadian Geotechnical Journal*, Vol. 21, No. 1, pp. 125-137.
- Burland, J. B. 1990. "On the compressibility and shear strength of natural clays," *Géotechnique*, Vol. 40, No. 3, pp. 329-378.

- DeGroot, D. J., Germaine, J. T. and Gedney, R. 1991. "An automated electropneumatic control system for direct simple shear testing," *ASTM Geotechnical Testing Journal*, Vol. 14, No. 4, pp. 339-348.
- Den Haan, E. J. and Kruse, G. A. M. 2007. "Characterisation and engineering properties of Dutch peats," *Proc. of Characterisation and Engineering Properties of Natural Soils, Singapore*, Vol. 3, pp. 2101-2133.
- Dyvik, R., Berre, T., Lacasse, S. and Raadim, B. 1987. "Comparison of truly undrained and constant volume direct simple shear tests," *Géotechnique*, Vol. 37, No. 1, pp. 3-10.
- Farrell, E. R. and Hebib, S. 1998. "The determination of the geotechnical parameters of organic soils," *Proceedings of International Symposium on Problematic Soils, IS-TOHOKU 98, Sendai, Japan*, Vol. pp. 33-36.
- Helenelund, K. V. 1967. "Vane tests and tension tests on fibrous peats," *Proc. Geotech. Conf. on shear strength properties of natural soils and rocks, Oslo*, Vol. 1, pp. 199-203.
- Hobbs, N. B. 1986. "Mire morphology and the properties and behaviour of some British and foreign peats," *Quarterly Journal of Engineering Geology and Hydrogeology*, Vol. 19, No. pp. 7-80.
- Kjellman, W. 1951. "Testing the shear strength of clay in Sweden," *Géotechnique*, Vol. 2, No. 3, pp. 225-232.
- Ladd, C. C. 1991. "Stability evaluation during staged construction," *Journal of Geotechnical Engineering Division ASCE*, Vol. 117, No. 4, pp. 540-615.
- Landva, A. O. 1980. "Vane testing in peat," *Canadian Geotechnical Journal*, Vol. 17, No. 1, pp. 1-19.

- Prevost, J. H. and Høeg, K. 1976. "Reanalysis of simple shear soil testing," *Canadian Geotechnical Journal*, Vol. 13, No. 4, pp. 418-429.
- Roscoe, K. H. 1953. "An apparatus for the application of simple shear to soil samples," *Proc of the 3rd Int. Conf. on Soil Mechanics and Foundation Engineering, London*, Vol. 1, pp. 186-191.
- von Post, L. and Granlund, E. 1926. "Peat resources in southern Sweden," *Sveriges geologiska undersökning, Yearbook*, Vol. 335, No. 19.2 Series C, pp. 1 – 127.
- White, D. J. and Take, W. A. 2005. "Discussion on: Application of Particle Image Velocimetry (PIV) in centrifuge testing of uniform clay," *International Journal of Physical Modelling in Geotechnics*, Vol. 5, No. 4, pp. 27-31.
- White, D. J., Take, W. A. and Bolton, M. D. 2003. "Soil deformation measurement using particle image velocimetry (PIV) and photogrammetry," *Géotechnique*, Vol. 53, No. 7, pp. 619-631.

TABLE 1 – Properties of clay for comparative tests

Moisture Content	35-37%
Bulk Density	1.8-2.0 Mg/m <sup>3</sup>
Plastic Limit (PL)	25%
Liquid Limit (LL)	39%

TABLE 2 – Properties of peat testing in UCD-DSS

Depth	0.4m-1.2m
Description	Fibrous Sphagnum Peat
Moisture Content	1300-1500%
Bulk Density	1.02 Mg/m <sup>3</sup>
Organic Content	95-99%
Decomposition <sup>a</sup>	H4/H5

<sup>a</sup> Decomposition measured according to method of Von Post and Granlund (1926) and detailed in Hobbs (1986)

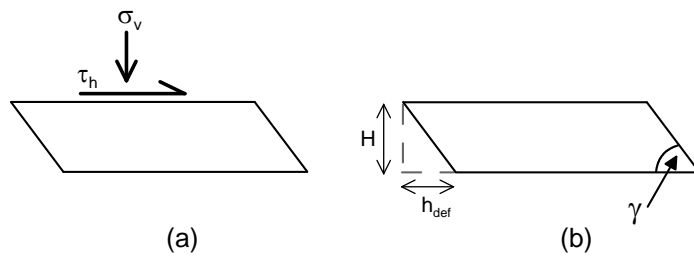


Figure 1 – Measurements in routine DSS tests (a) Stress (b) Deformations

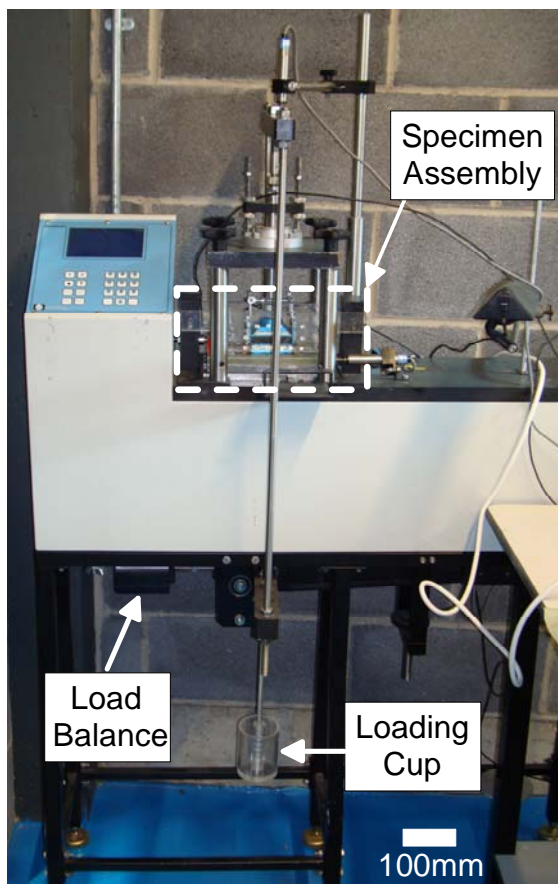


Figure 2 – Overview photograph of UCD-DSS apparatus



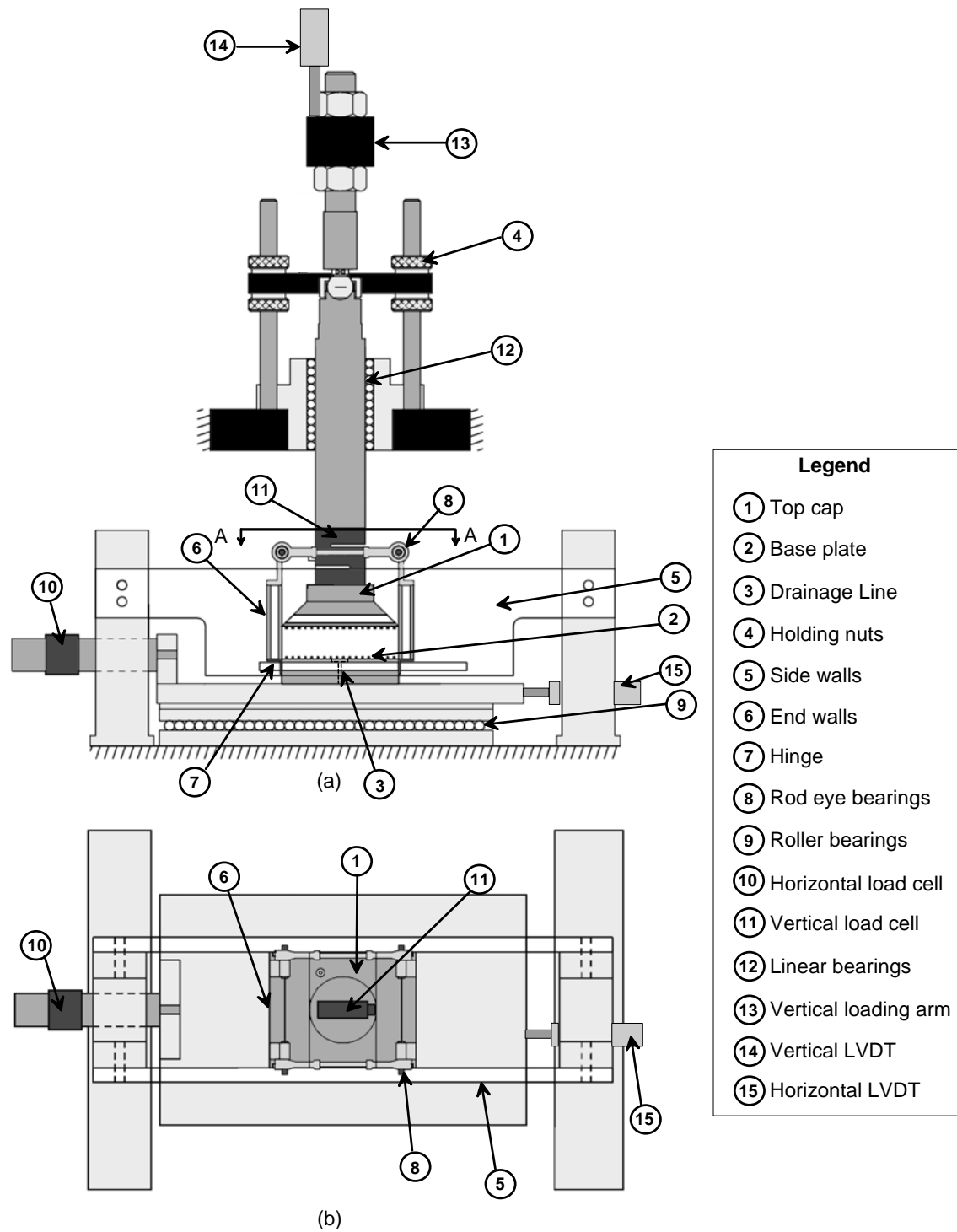


Figure 3 – (a) Side view of test specimen assembly of UCD-DSS apparatus (b) Section A-A overview

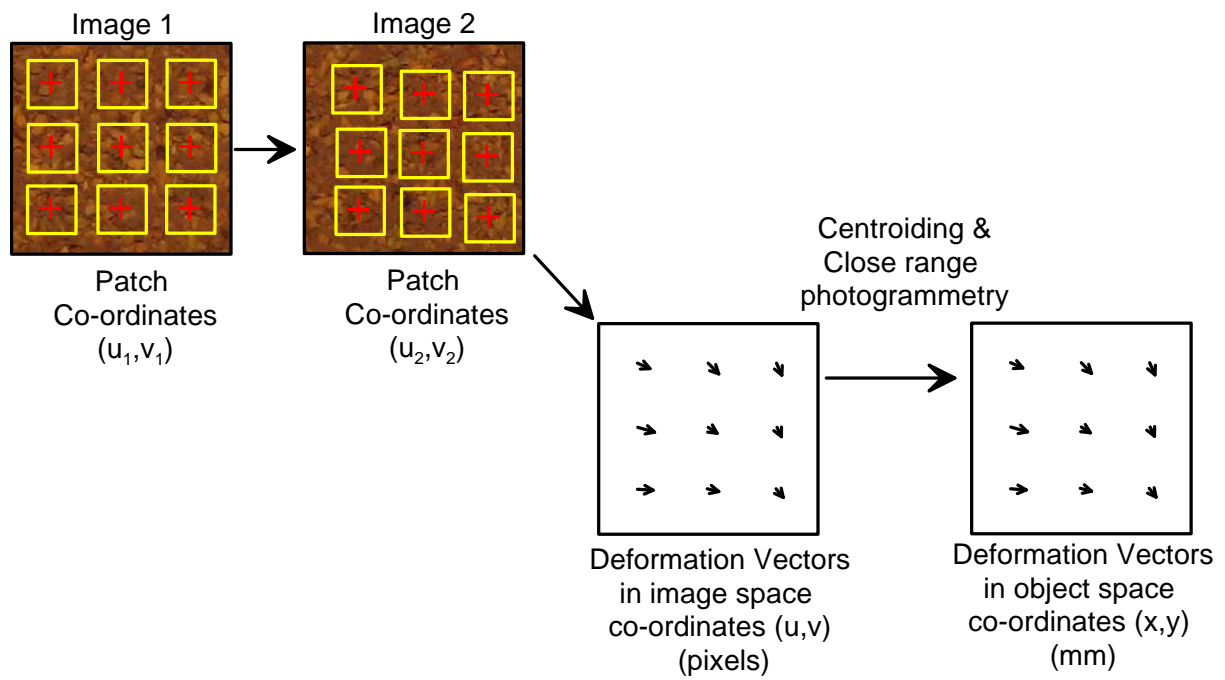


Figure 4 – GeoPIV process

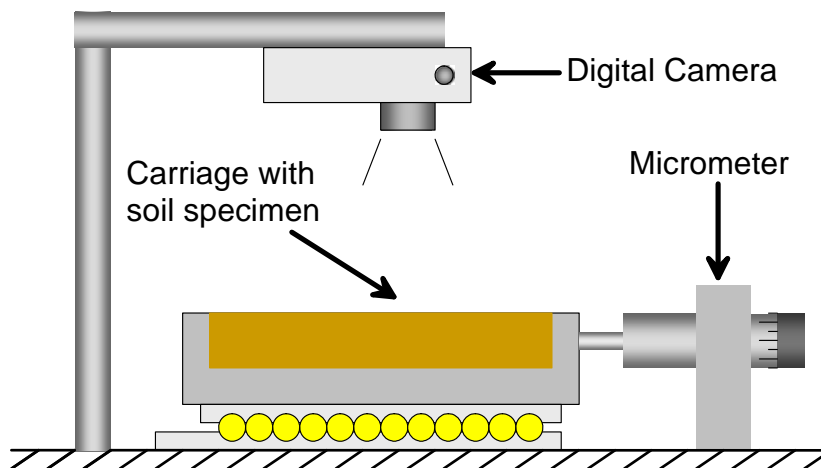


Figure 5 – Experimental setup for PIV precision tests

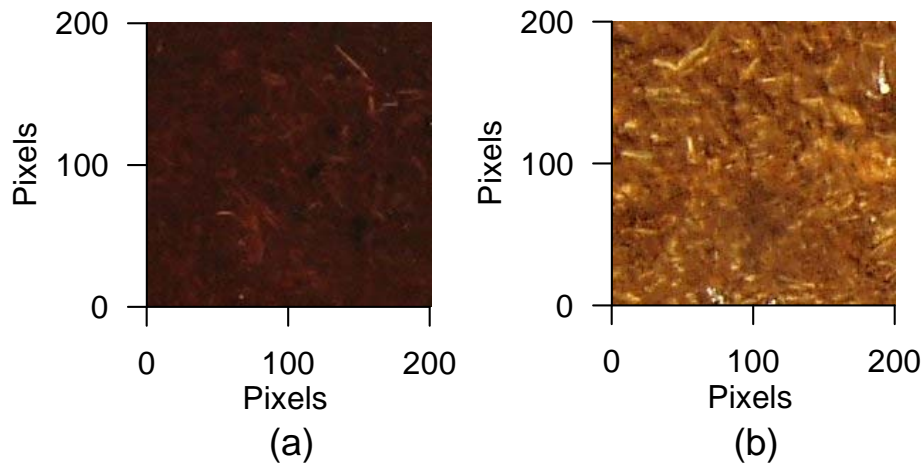


Figure 6 – Peat specimens for PIV precision tests

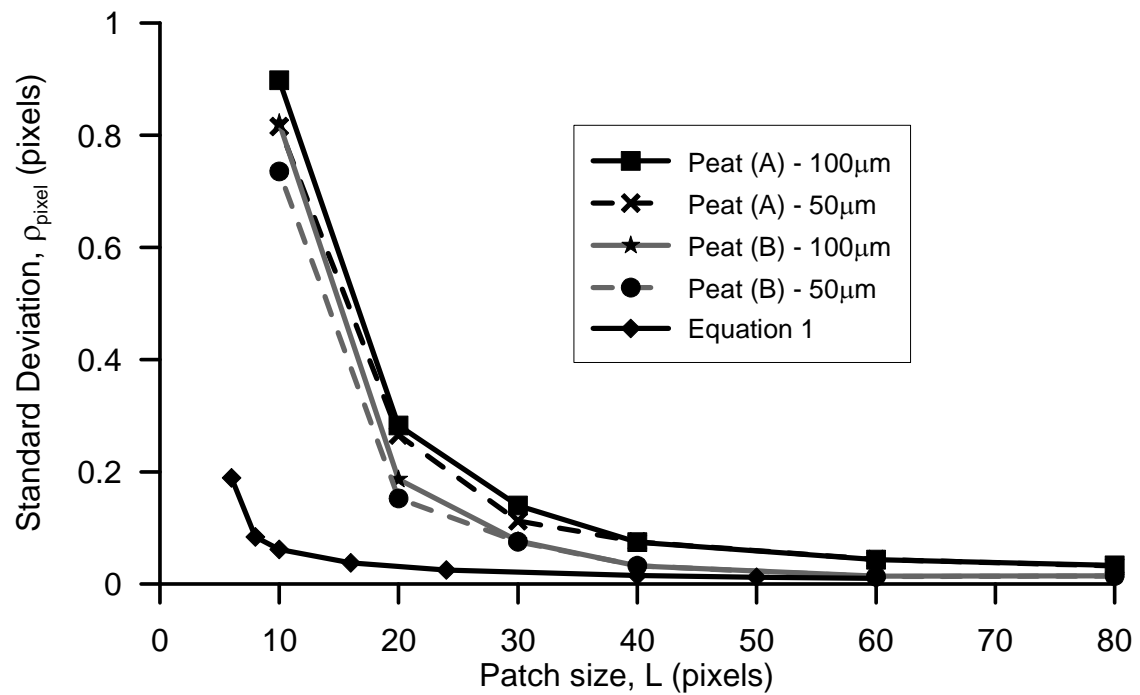


Figure 7 – Effect of patch size and material contrast on PIV analyses of peat

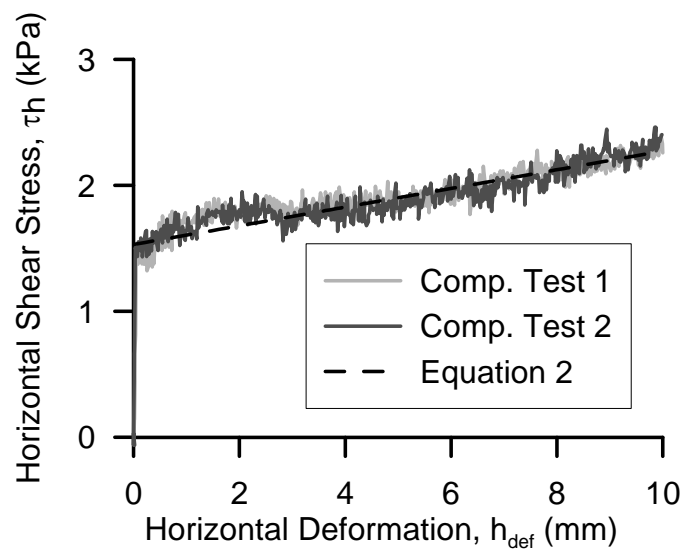


Figure 8 – Horizontal compliance test

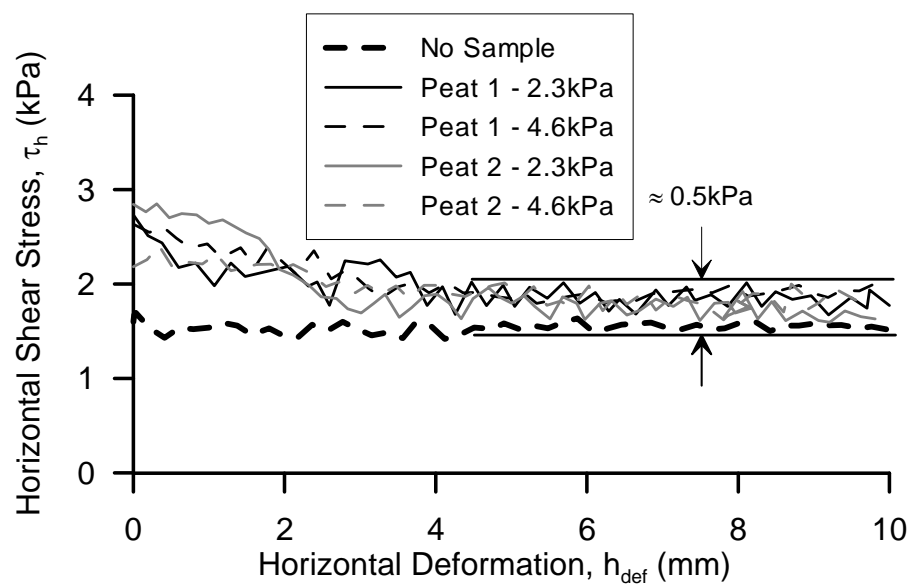


Figure 9 – Measurement of side wall friction

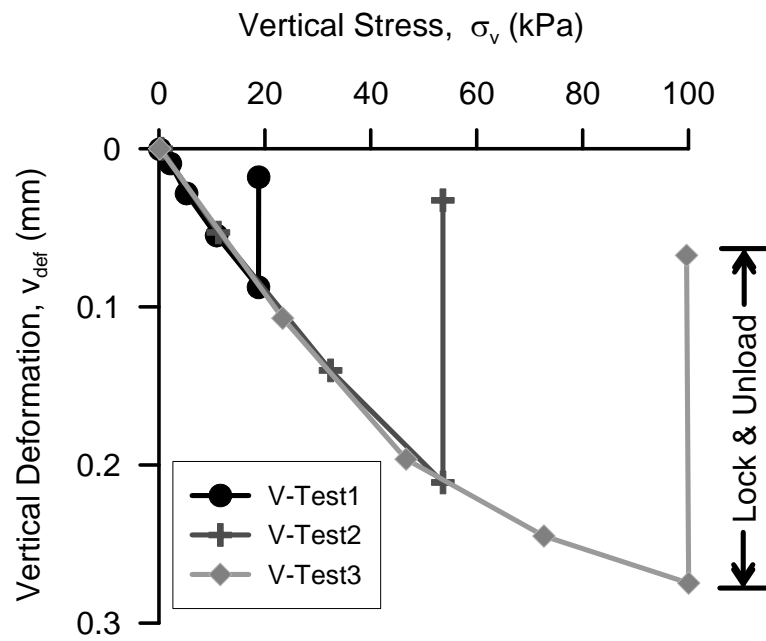


Figure 10 – Vertical compliance tests

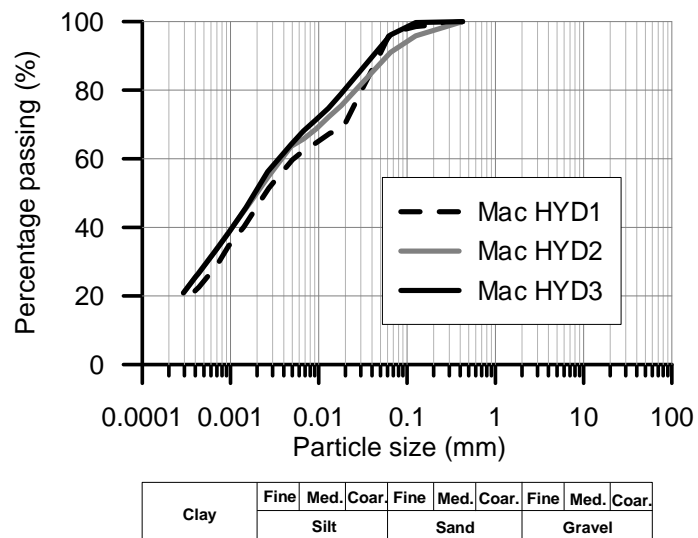


Figure 11 – Particle size distribution (PSD) of clay for comparative tests

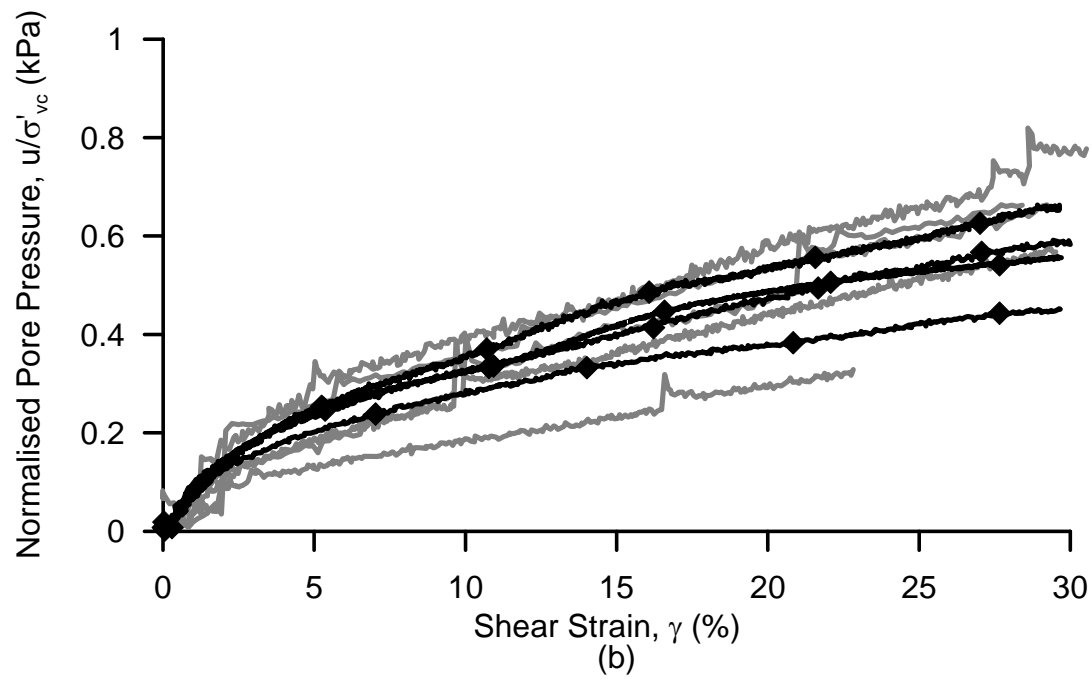
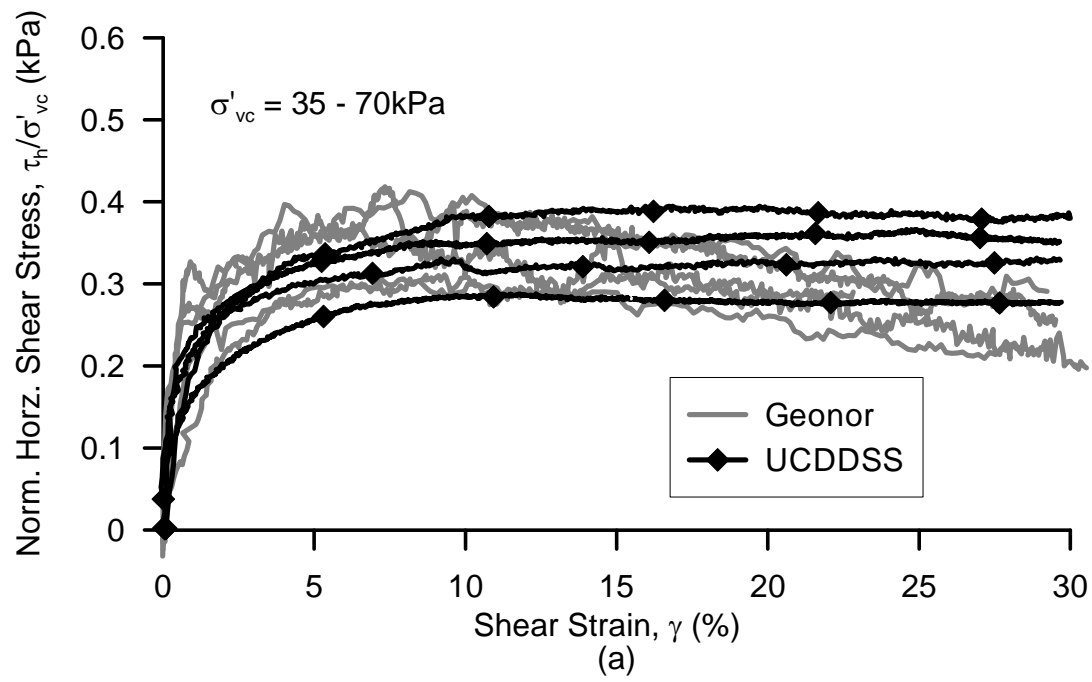


Figure 12 – (a) Normalised horizontal shear stress (b) Normalised pore pressure versus shear strain for all comparative DSS tests

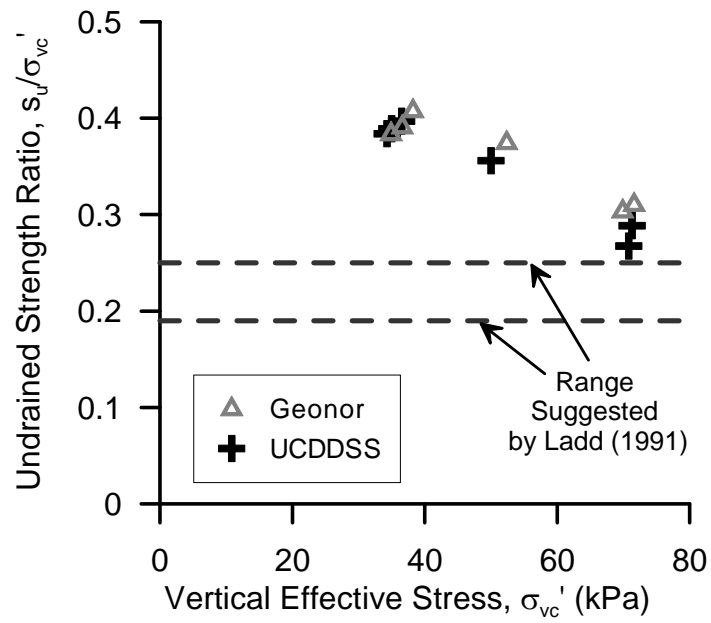


Figure 13 – Undrained shear strength ratios for all DSS tests

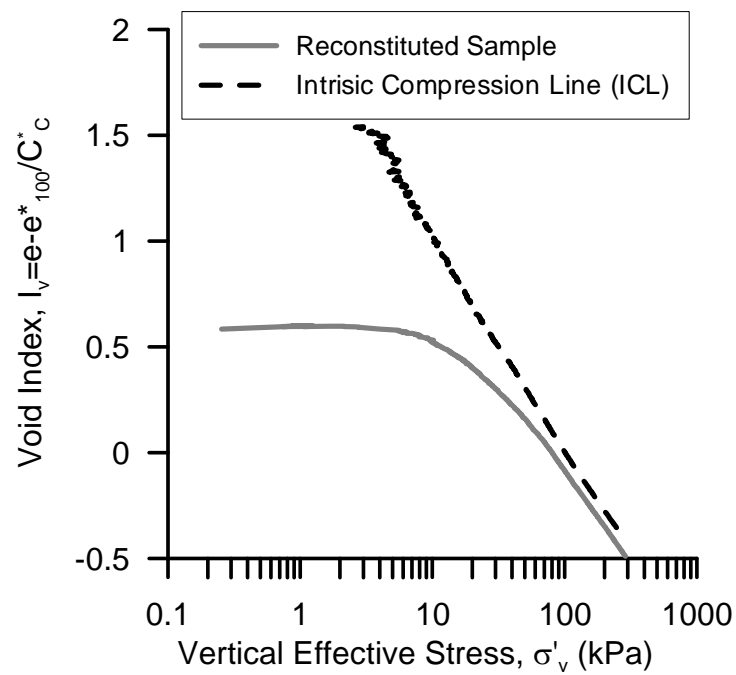


Figure 14 – Constant rate of strain (CRS) oedometer test results

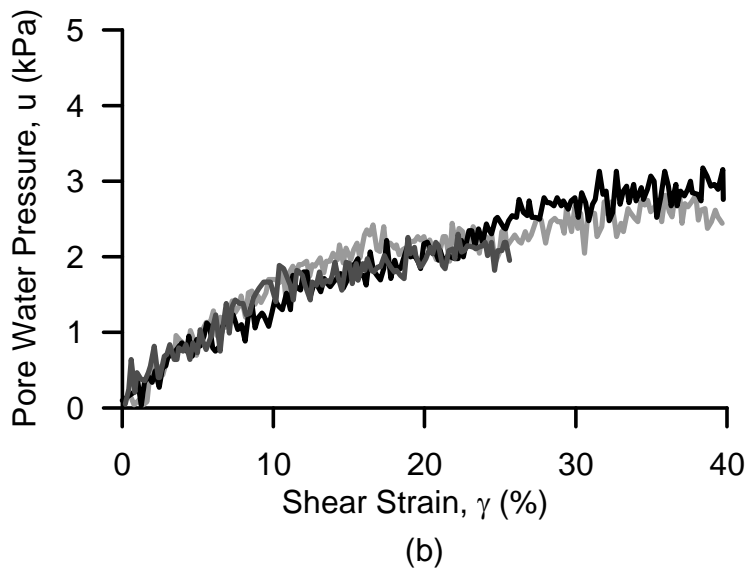
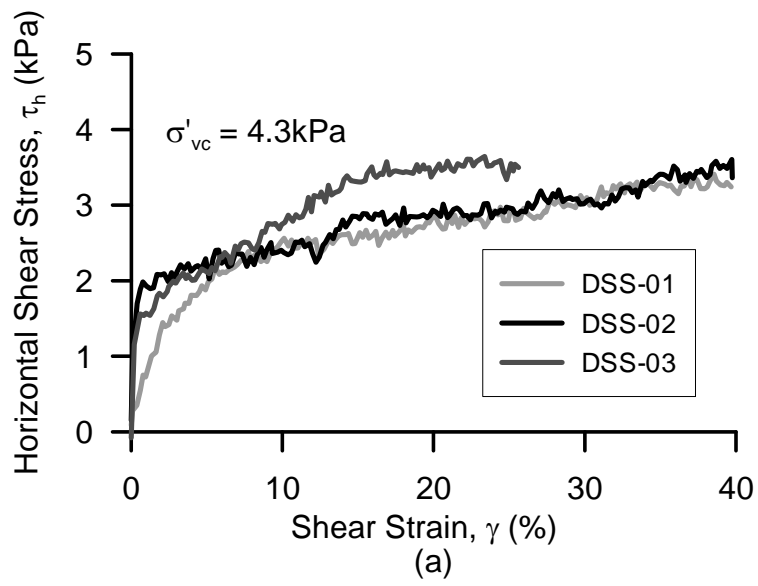


Figure 15 – (a) Horizontal shear stress (b) Pore pressure versus shear strain for Loughrea DSS tests



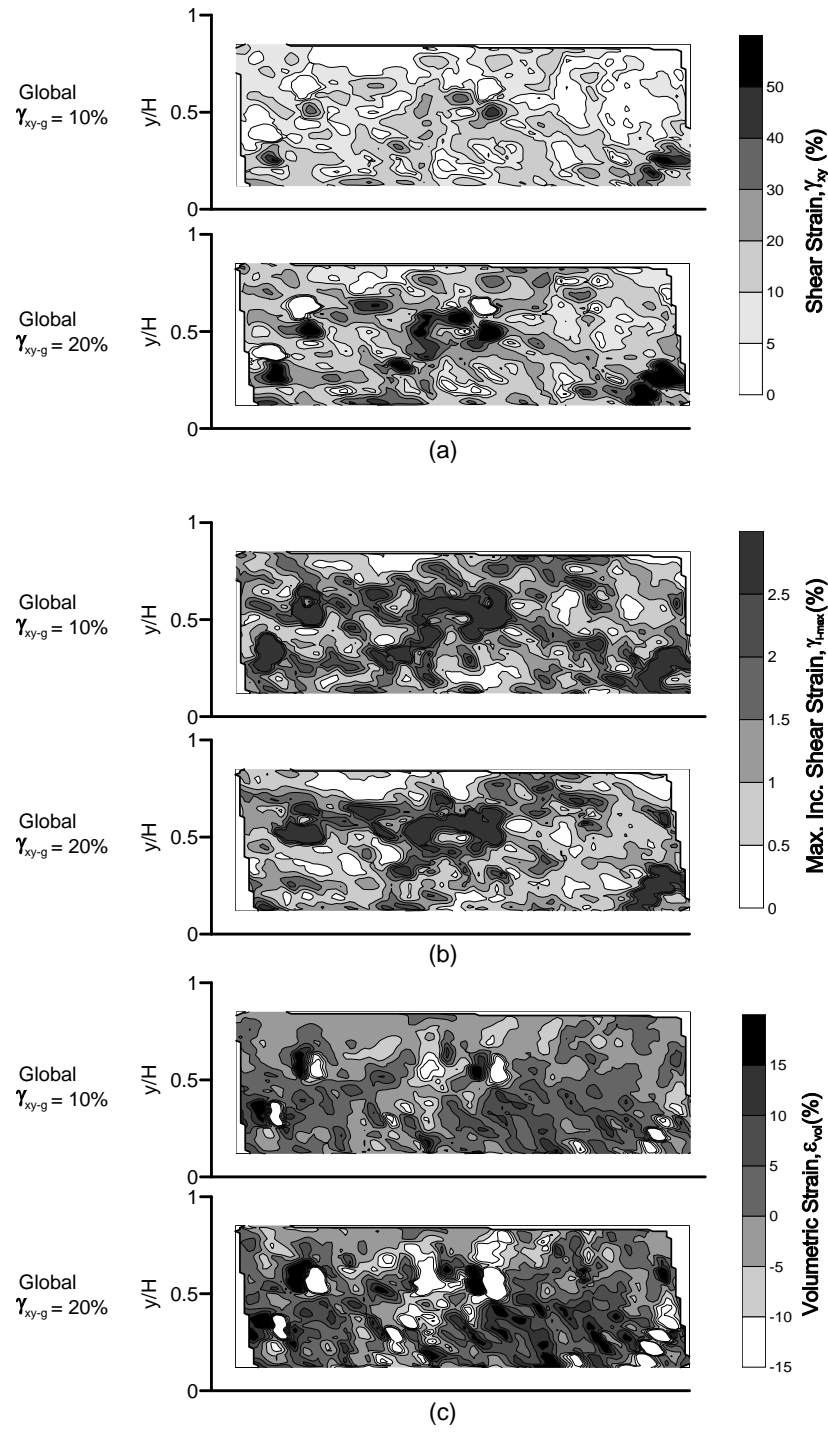


Figure 16 – DSS-01, Distributions of (a) Engineering Shear Strains (b) Maximum incremental shear strains (c) Volumetric Strains

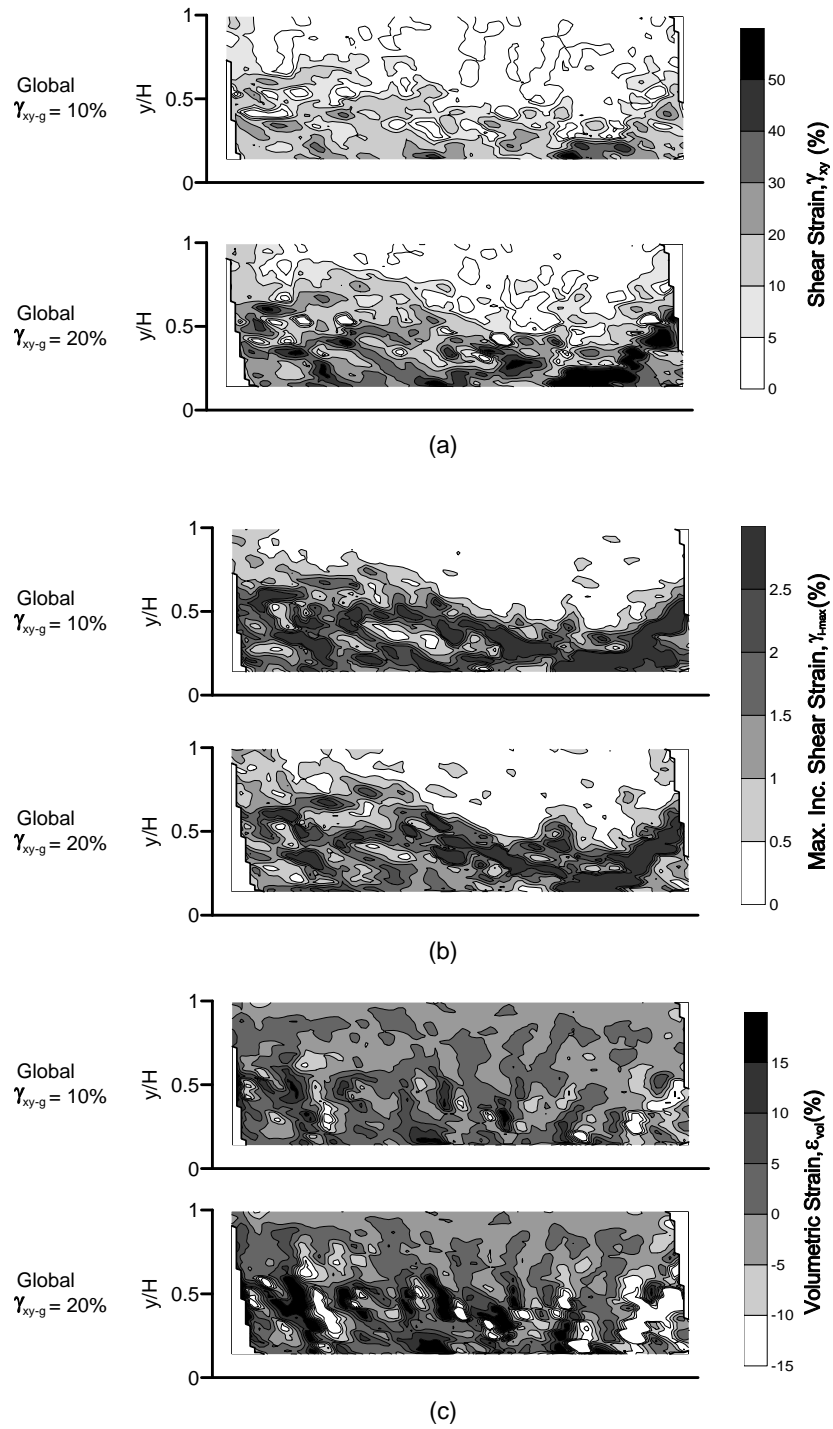


Figure 17 – DSS-02, Distributions of (a) Engineering Shear Strains (b) Maximum incremental shear strains (c) Volumetric Strains